Electronic structure and vibrational entropies of fcc Au-Fe alloys

J. A. Muñoz,[1] M. S. Lucas,[2,3] L. Mauger,[1] I. Halevy,[1] J. Horwath,[2] S. L. Semiatin,[2] Yuming Xiao,[4] Paul Chow,[4] M. B. Stone,[5] D. L. Abernathy,[5] and B. Fultz[1]

[1]*California Institute of Technology, W. M. Keck Laboratory 138-78, Pasadena, California 91125, USA*

[2]*Air Force Research Laboratory, Wright-Patterson AFB, Ohio 45433, USA*

[3]*UTC Inc., 1270 North Fairfield Road, Dayton, Ohio 45432, USA*

[4]*HPCAT, Geophysical Laboratory, Carnegie Institute of Washington, Argonne, Illinois 60439, USA*

[5]*Oak Ridge National Laboratory, 1 Bethel Valley Road, Oak Ridge, Tennessee 37831, USA*

(Received 13 September 2012; revised manuscript received 12 November 2012; published 10 January 2013)

Phonon density of states (DOS) curves were measured on alloys of face-centered-cubic (fcc) Au-Fe using nuclear resonant inelastic x-ray scattering (NRIXS) and inelastic neutron scattering (INS). The NRIXS and INS results were combined to obtain the total phonon DOS and the partial phonon DOS curves of Au and Fe atoms from which vibrational entropies were calculated. The main effect on the vibrational entropy of alloying comes from a stiffening of the Au partial phonon DOS with Fe concentration. Force constants were calculated from first principles for several compositions and show a local stiffening of Au-Au bonds close to Fe atoms. The calculated phonon DOS curves reproduce the experimental trend. The stiffening is attributed to two main effects comparable in magnitude: (i) an increase in electron density in the free-electron-like states and (ii) stronger *sd* hybridization.

DOI: 10.1103/PhysRevB.87.014301 PACS number(s): 63.20.dd, 63.20.Pw, 71.20.Be, 75.50.Bb

I. INTRODUCTION

Iron and gold are ubiquitous in modern materials technology. Au-Fe alloys have interesting magnetic properties, where Fe atoms can have larger magnetic moments than in pure Fe,[1] and magnetism can stabilize pseudomorphic Au-Fe mixtures on surfaces.[2] Nanoparticles of Au-Fe alloys[3–6] are promising for cancer treatment applications[7] owing to the biocompatibility of Au.[8] Nevertheless, mixtures of Au and Fe atoms are uncommon because these elements are largely immiscible at low temperatures. Although Fe is widely soluble in face-centered cubic (fcc) Au at elevated temperatures and quenching can preserve Au-Fe solid solutions, the solubility of Au in body-centered cubic (bcc) Fe is low, presumably because of the comparably large atomic volume of Au.

The phonon spectra of Au-Fe alloys provide information on the local atomic forces and on the vibrational entropy. An early Mössbauer spectrometry study assessed the force constant of Fe impurities in fcc Au[9] using the impurity model developed by Mannheim.[10] Recent studies on Au-Fe alloys have investigated the phonon spectra of Fe atoms in multilayers[11,12] and nanoclusters[13] using the technique of nuclear resonant inelastic x-ray scattering (NRIXS), which probes only the motions of Fe atoms.

For binary Fe-*X* alloys, combining NRIXS with inelastic neutron scattering (INS) allows determination of the partial phonon DOS of the Fe atoms, the partial phonon DOS of the *X* atoms, and the total phonon DOS of the alloy. Such measurements provide very detailed information on the role of phonons in alloy thermodynamics.[14] For example, with data over a range of chemical compositions, it was shown how local atomic arrangements alter the vibrational entropy of Fe-V,[15,16] Fe-Cr,[17,18] and Fe-Co[19] alloys.

No direct measurements of the phonons of Fe atoms in bulk Au-Fe alloys have been performed to date. Measurements of phonons in Au-Fe alloys are challenged by the x-ray and neutron absorbing properties of Au. Nevertheless, INS measurements have been performed with direct geometry chopper spectrometers,[20,21] and modern instruments make such measurements more practical.[22,23] In the present study using NRIXS and INS, we identified the local modes of Fe atoms in an fcc Au host. We investigated how both Fe and Au vibrations changed with increasing Fe composition, and the effects of both species on the vibrational entropy of the solid solution. First-principles calculations of the force constants and electronic structures of Au-Fe compounds were used to interpret the phonon DOS curves. The phonon partial DOS of Au atoms depends strongly on the Fe concentration, with an increase in energy (stiffening) of the Au vibrations with increasing Fe content. This stiffening of the Au modes dominates the alloy vibrational entropy but, contrary to transition metal alloys,[15,16,24,25] cannot be fully explained by changes in lattice parameter or the overall electronic DOS at the Fermi level. We suggest that its origin is twofold. First, the donation of charge from Fe atoms to a nearly-free electronic band causes a stiffening of the elastic constants. Second, the increase in the number of available *d* electrons from the Fe affects the *sd* hybridization and, according to the Wills-Harrison model,[26] results in stiffer bonds.

II. EXPERIMENTAL

Alloys of stoichiometric $Au_{1-x_{Fe}}Fe_{x_{Fe}}$ with nominal compositions $x_{Fe} = 0.03, 0.10, 0.20, 0.30, 0.40, 0.50, 0.60$ were prepared from Fe metal enriched 96.06% in ^{57}Fe and 99.999% Au by arc-melting under an argon atmosphere. Electron microprobe measurements confirmed the compositions to be accurate to 0.6 at.%. The ingots were cold rolled to thicknesses between 10 and 50 μm. To remove strains, the foils were sealed in quartz tubes, annealed, and quenched into iced brine. All samples were annealed at temperatures between 950 and 1110 °C for 30 minutes. Higher temperatures were used for higher Fe concentrations to avoid forming the bcc phase.[27] X-ray diffractometry showed all samples to be single-phase fcc. The lattice parameter was found to decrease with

TABLE I. Measured lattice parameter a and vibrational entropy S_{vib} of Au-Fe alloys at 300 K from x-ray diffraction, nuclear resonant inelastic x-ray scattering, and inelastic neutron scattering. S_{vib}^{Fe} and S_{vib}^{Au} denote the vibrational entropy of the Fe and Au atoms, S_{vib}^{NW} is the average vibrational entropy per atom as obtained from the neutron-weighted INS data, and S_{vib} is the neutron-weight corrected average entropy per atom obtained by combining the INS and NRIXS results as described in the text. Errors from counting statistics.

Sample	a (x-ray) ± 0.002 Å	a (neutron) ± 0.008 Å	S_{vib}^{Fe} k_B per atom	S_{vib}^{Au} k_B per atom	S_{vib}^{NW} ± 0.01 k_B per atom	S_{vib} k_B per atom
Au	4.0786	4.0693	...	5.64 ± 0.01	5.64	5.64 ± 0.01
$Au_{0.97}Fe_{0.03}$	4.0721	4.0638	4.19 ± 0.06	5.56 ± 0.02	5.36	5.52 ± 0.02
$Au_{0.90}Fe_{0.10}$	4.0555	...	4.19 ± 0.05	...	...	...
$Au_{0.80}Fe_{0.20}$	4.0262	4.0256	4.21 ± 0.04	5.07 ± 0.06	4.58	4.89 ± 0.05
$Au_{0.70}Fe_{0.30}$	3.9913	...	4.13 ± 0.04	...	...	...
$Au_{0.60}Fe_{0.40}$	3.9492	...	4.07 ± 0.03	...	...	...
$Au_{0.50}Fe_{0.50}$	3.9084	3.9001	3.97 ± 0.03	5.36 ± 0.17	4.19	4.67 ± 0.09
$Au_{0.40}Fe_{0.60}$	3.8607	...	3.96 ± 0.03	...	...	...

increasing Fe concentration (see Table I) in good agreement with previous results.[28–30] The magnetization was measured with a vibrating sample magnetometer (VSM) up to an applied field of 2 T. Transmission Mössbauer spectrometry was performed with a conventional constant acceleration spectrometer. Both the VSM and Mössbauer results indicate that at room temperature the samples with compositions $x_{Fe} = 0.03$, 0.10, and 0.20 are paramagnetic with no Fe clustering and the samples with higher Fe concentration are ferromagnetic. The magnetic properties are consistent with previous results,[1] as are the room-temperature Mössbauer spectra.[31]

NRIXS[32–34] was performed at beamline 16ID-D[22] at the Advanced Photon Source (APS) of the Argonne National Laboratory. All measurements were performed at room temperature. The monochromator resolution function was 2.2-meV FWHM. More details about the experimental procedures can be found in a recent article.[19] The NRIXS data were reduced with the software PHOENIX[35] and the results are presented in Fig. 1.

INS measurements on alloys of compositions $x_{Fe} = 0$, 0.03, 0.20, 0.50 were performed with the ARCS spectrometer[23] at the Spallation Neutron Source (SNS) at the Oak Ridge National Laboratory. These samples were prepared from Fe of natural isotopic abundance by the same procedures as for the NRIXS samples, and were cold rolled into 120-μm thick foils and given the same heat treatments. The measurements were performed at room temperature at an incident neutron energy of 40 meV. At this energy, the instrument resolution is 1.6-meV FWHM at the elastic line, although the energy resolution of a direct geometry spectrometer improves with increasing energy transfer. Details of the data collection and reduction procedures are described elsewhere.[18,36–38] The resulting neutron-weighted phonon DOS curves are shown in Figs. 2(top) and 3. The phonon DOS for pure Au was

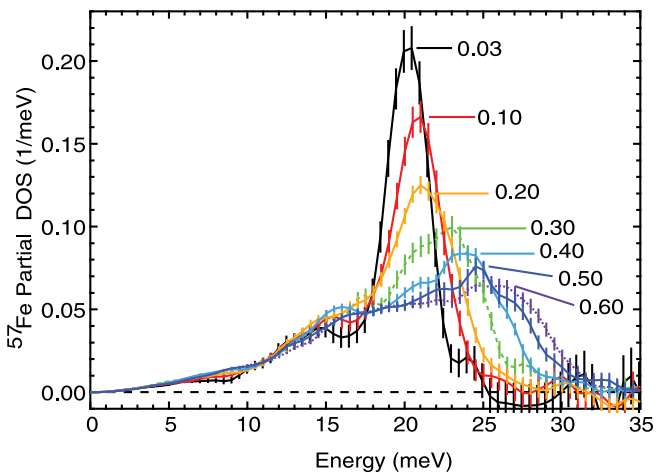

FIG. 1. (Color online) ^{57}Fe partial phonon DOS curves, $g^{Fe}(E)$, for the $Au_{1-x_{Fe}}Fe_{x_{Fe}}$ alloys at 300 K from NRIXS measurements. The Fe content x_{Fe} for each curve is indicated in the figure.

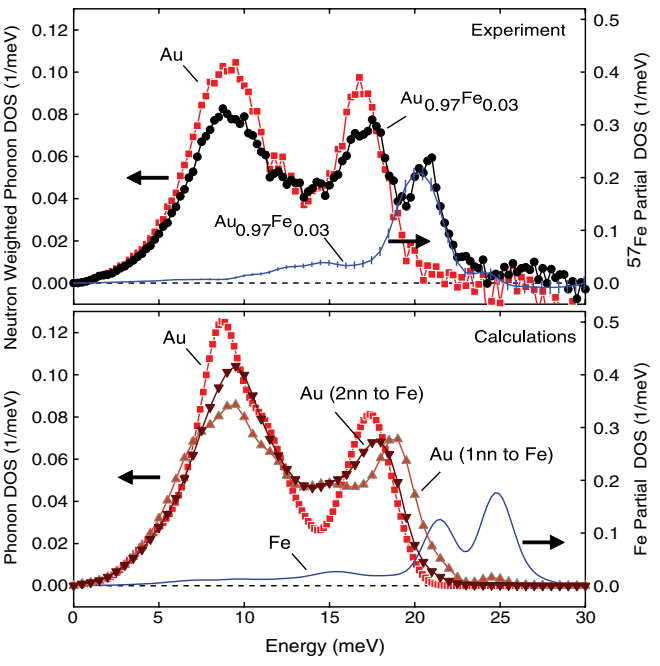

FIG. 2. (Color online) Experimental (top) and calculated (bottom panel) phonon DOS curves. (Top) Left axis is the neutron-weighted phonon DOS curves for pure Au and $Au_{0.97}Fe_{0.03}$ from INS measurements and the right axis is the ^{57}Fe partial phonon densities of states for $Au_{0.97}{}^{57}Fe_{0.03}$ from NRIXS measurements. Analogous curves were calculated for pure Au and an SQS of $Au_{30}Fe_2$, but the motions of Au atoms that are 1nn to a Fe atom and those that are 2nn are plotted separately.

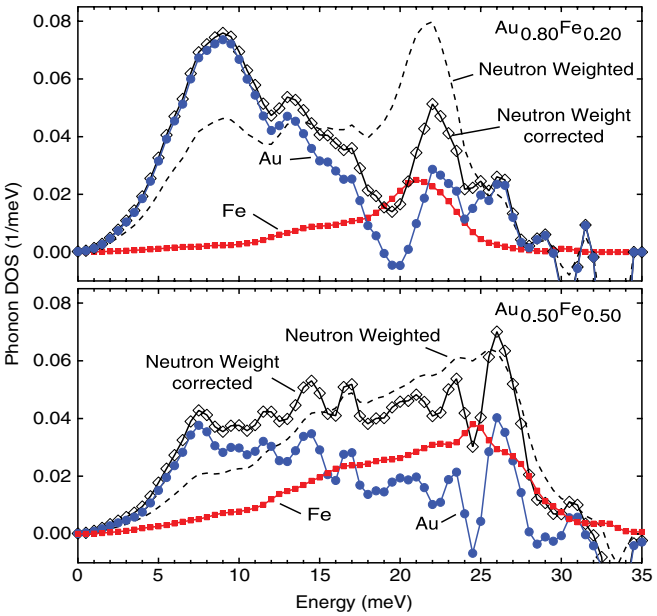

FIG. 3. (Color online) Neutron-weighted (dashed curves without markers) and neutron-weight-corrected (open diamonds) phonon DOS curves, along with the concentration weighted Fe (solid squares) and Au (solid circles) partial phonon DOS curves for $Au_{0.80}Fe_{0.20}$ (top) and $Au_{0.50}Fe_{0.50}$ (bottom).

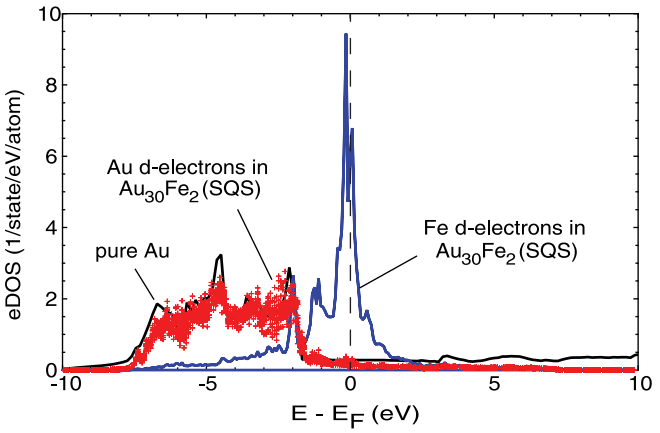

FIG. 4. (Color online) Calculated electronic DOS curves for d electrons in the SQS of paramagnetic $Au_{30}Fe_2$ at the Fe and Au sites and electronic DOS of pure Au. The vertical line marks the Fermi energy.

in excellent agreement with the triple axis measurement of Lynn *et al.*[39] after convolution with the experimental resolution function.

III. COMPUTATIONAL

Total energy and force calculations were performed with density functional theory (DFT) on fcc Au, an fcc structure with 1 Fe atom and 31 Au atoms, a $L1_2$ ordered structure of Au_3Fe, and four 32-atom special quasirandom structures (SQSs) with 2, 4, 6, and 8 Fe atoms, respectively. An SQS is a specially designed periodic structure with the same values of atomic correlation functions (in the cluster expansion formalism[40,41]) as the random solid solution.[42] We used the SQSs of von Pezold *et al.*[43]

We used the package VASP[44,45] with projector-augmented wave (PAW) potentials with the local density approximation (LDA) exchange-correlation[46,47] functional. The electronic structure was calculated for pure Au and $L1_2$ Au_3Fe using four-atom unit cells using a $24 \times 24 \times 24$ k-point mesh generated with the Monkhorst-Pack scheme[48] and a plane wave kinetic energy cutoff of 450 eV. For the structures with 32 atoms, the k-point mesh consisted $8 \times 8 \times 8$ k points and the kinetic energy cutoff was 500 eV. In all cases, the total energy converged to less than 1 meV. The calculations were spin-polarized in the cases of the SQS of $Au_{24}Fe_8$ and Au_3Fe, which are ferromagnetic at room temperature, giving magnetic moments of 2.75 and 3.00 μ_B/Fe atom, respectively, which are comparable to the value of 2.9 μ_B/Fe atom measured on a solid solution of the same composition.[1] The ground-state lattice parameter in each case was found by fitting the energy-volume relationship to the third-order Birch-Murnaghan equation of state, giving results within a few percent of the experimental values and reproducing the trend observed in Table I. Electronic DOS curves for pure Au and the d electrons of the SQS structure of paramagnetic $Au_{30}Fe_2$ are shown in Fig. 4.

To calculate the interatomic force constants for pure Au and Au_3Fe, we used a 108-atom supercell ($3 \times 3 \times 3$ times the standard fcc unit cell) and a $3 \times 3 \times 3$ k-point mesh. For $Au_{31}Fe_1$ and the SQS structure of $Au_{30}Fe_2$, we used a 256-atom supercell ($4 \times 4 \times 4$ times the conventional fcc unit cell) and a $2 \times 2 \times 2$ k-point mesh. In all cases, the atom displacements were 0.01 Å. The grid used to store the wave function and charge density coefficients (basicGrid) included all wave vectors up to twice the cutoff energy to avoid wrap-around errors, and the grid used to calculate the augmentation charges was eight times denser than the basicGrid. This is necessary for accurate thermodynamic calculations.[49] Force constants were calculated by the Parlinski-Li-Kawazoe method[50] as implemented in the PHONOPY code[51] and, in the case of pure Au, were found to be in good agreement with both experimental fits[39] and calculated results.[52,53] The elements of the interatomic force constant tensor and the resulting bond stretching force constant are listed in Table II. Dynamical matrices were calculated from the force constants, and phonon DOS curves were computed on $16 \times 16 \times 16$ q-point meshes using the Monkhorst-Pack scheme.[48] Results for pure Au and the SQS of $Au_{30}Fe_2$ are shown in the bottom panel of Fig. 2.

IV. RESULTS

Different elements have different neutron scattering efficiencies, so data obtained from INS are neutron-weighted. The neutron weights are the ratios of neutron cross section to molar mass, σ/M, which are 0.208 and 0.039 barns/amu for Fe and Au, respectively, so the motions of Fe atoms are overemphasized by a 5:1 ratio. A neutron-weight correction was made possible by combining the INS neutron-weighted phonon DOS spectra with the NRIXS Fe partial phonon DOS spectra.[15]

TABLE II. Interatomic force constant tensor elements and bond-stretching (longitudinal) force constants for pure Au, ordered $Au_{31}Fe_1$ and $L1_2$ Au_3Fe, and the SQS of $Au_{30}Fe_2$ from first-principles calculations for first-, second-, and third-nearest neighbors (1nn, 2nn, and 3nn, respectively). For the longitudinal force constants, denoted by ϕ_{zz}, the bond direction was rotated to be along the z axis by covariant transformation. For $Au_{31}Fe_1$, the values reported for the Au-Au bonds are for Au atoms that have at least one Fe atom as a 1nn. The forces reported for the SQS of $Au_{30}Fe_2$ are average forces and two sets of Au-Au forces are given, one for Au atoms that have a Fe atom as a 1nn and another for Au atoms that are 2nn to Fe atoms. All force constants have units of N/m.

		Au	$Au_{31}Fe_1$		Au_3Fe			$Au_{30}Fe_2$ (SQS)		
		Au-Au	Au-Au[a]	Fe-Au	Au-Au	Fe-Au	Fe-Fe	Au-Au[a]	Au-Au[b]	Fe-Au
1nn	ϕ_{11}	16.63	18.43	5.49	23.15	7.39	...	...	...	...
	ϕ_{12}	20.82	23.43	5.78	26.88	12.65	...	...	...	...
	ϕ_{33}	−8.62	−7.16	−0.38	−12.46	−2.67	...	...	...	...
	ϕ_{zz}	37.44	41.86	11.27	50.04	20.04	...	45.80	36.57	20.76
2nn	ϕ_{11}	4.90	4.52	2.64	3.59	...	0.63	...	...	...
	ϕ_{22}	0.07	0.81	−0.88	0.09	...	0.89	...	...	...
	ϕ_{zz}	4.90	4.52	2.64	3.59	...	0.63	4.05	4.42	2.84
3nn	ϕ_{11}	1.07	1.16	0.26	1.82	0.69	...	...	...	...
	ϕ_{22}	1.01	1.06	0.01	1.38	0.07	...	...	...	...
	ϕ_{12}	0.43	0.53	0.58	1.25	−0.11	...	...	...	...
	ϕ_{23}	0.12	−0.15	0.00	−2.06	0.24	...	...	...	...
	ϕ_{zz}	1.59	1.67	0.62	4.15	0.59	...	0.53	0.58	1.25

[a]Au-Au bonds that have at least one Fe atom as a first-nearest neighbor.
[b]Au-Au bonds that have at least one Fe atom as a second-nearest neighbor and no Fe atoms as a first-nearest neighbor.

The vibrational entropy $S_{\rm vib}$ is obtained from $g(E)$,[54] the normalized phonon DOS,

$$S_{\rm vib} = 3k_B \int g(E)[(n+1)\ln(n+1) - n\ln(n)]dE\ , \quad (1)$$

where n is the Planck distribution and the integral is from zero to the cutoff energy. The excess vibrational entropy of mixing as a function of Fe concentration $x_{\rm Fe}$ due to motions of atoms of type $d = \{\rm Au, Fe\}$ in $Au_{1-x_{\rm Fe}}Fe_{x_{\rm Fe}}$ is

$$\Delta S^d_{\rm vib}(x_{\rm Fe}) = S^d_{\rm vib}(x_{\rm Fe}) - \mathcal{S}^d_{\rm vib}\ , \quad (2)$$

where $\mathcal{S}^d_{\rm vib}$ is the vibrational entropy of pure element d. As shown in Table I, $\mathcal{S}^{\rm Au}_{\rm vib} = 5.64\ k_{\rm B}$ per atom, but fcc Fe is not stable at room temperature, so we use $\mathcal{S}^{\rm Fe}_{\rm vib} = 3.50\ k_{\rm B}$ per atom, which is the phonon entropy of ^{57}Fe in $Ni_{0.50}{}^{57}Fe_{0.50}$ from NRIXS measurements at 300 K.[55] Phonon DOS curves of solid solutions of fcc Ni-Fe, and therefore their vibrational entropies, do not change much with composition[56] and are in very good agreement with those of fcc Fe precipitates in Cu,[57] pseudomorphic fcc Fe films,[58] and fcc Fe at high temperature.[59] We expect the true $\mathcal{S}^{\rm Fe}_{\rm vib}$ to be $3.5 \pm 0.3\ k_{\rm B}$ per atom, with a conservative range estimate, but corrections of this magnitude do not substantially change the values of the excess vibrational entropy of mixing for Au-Fe alloys shown in Fig. 5. The excess vibrational entropy of mixing for the alloy $Au_{1-x_{\rm Fe}}Fe_{x_{\rm Fe}}$ is the concentration-weighted sum of the curves obtained from Eq. (2) for Au and Fe motions:

$$\Delta S_{\rm vib}(x_{\rm Fe}) = (1-x_{\rm Fe})\ \Delta S^{\rm Au}_{\rm vib}(x_{\rm Fe}) + x_{\rm Fe}\ \Delta S^{\rm Fe}_{\rm vib}(x_{\rm Fe}). \quad (3)$$

The neutron-weighted phonon DOS of $Au_{0.97}Fe_{0.03}$ is presented in the top panel of Fig. 2 along with the measured partial phonon DOS of the Fe modes. Both curves are normalized, but the vertical axes were adjusted to emphasize that the peak centered at 20.1 meV is mainly due to a local Fe mode. This value is 4.3% higher than the pure Au cutoff energy, $E_c = 19.3$ meV.[39] The general shape of the Au partial phonon DOS of $Au_{0.97}Fe_{0.03}$ does not differ much from that of pure Au. There is a very small stiffening due to the reduction in lattice parameter and the transverse and longitudinal peaks are centered at the same energies. Nevertheless, there is some intensity at energies higher than E_c, in the region where the Fe mode is located, and this intensity is the main contribution to the reduction in vibrational entropy in $Au_{0.97}Fe_{0.03}$ with respect to pure Au.

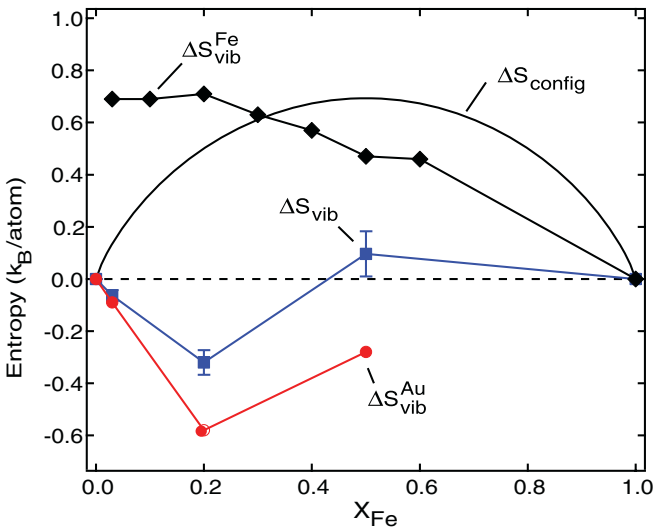

FIG. 5. (Color online) Configurational entropy of mixing ($\Delta S_{\rm config}$) and excess vibrational entropy of mixing ($\Delta S_{\rm vib}$) for $Au_{1-x_{\rm Fe}}Fe_{x_{\rm Fe}}$ alloys with respect to ideal mixing of fcc Au and fcc Fe. Excess vibrational entropy contributions from Au and Fe are $\Delta S^{\rm Au}_{\rm vib}$ and $\Delta S^{\rm Fe}_{\rm vib}$.

The bottom panel of Fig. 2 shows the calculated phonon DOS for pure Au and the partial phonon DOS curves of Au and Fe in an SQS of $Au_{30}Fe_2$. The Au motions in the SQS are further separated into those of Au atoms that have Fe atom as 1nn and Au atoms that have a Fe atom as a second-nearest neighbor (2nn) but not as a first-nearest neighbor (1nn). Although the composition is slightly higher than in the experimental sample, the trends are satisfactorily reproduced. The Fe modes are mostly at energies higher than the calculated value of E_c, which is in agreement with the experimental results. There is some intensity in the Au partial phonon DOS of $Au_{0.97}Fe_{0.03}$ in the same energy range. There is also some stiffening of the rest of the Au modes with respect to pure Au, consistent with a decrease in lattice parameter, although the motions of Au atoms close to Fe atoms are affected more by the decrease in lattice parameter. The Au vibrations with energies greater than E_c come from Au atoms that are 1nn to a Fe atom. This can also be seen in Table II, which shows that the Au-Au bonds that have at least one Fe atom as the nearest neighbor are substantially stiffer than those that are farther away from Fe atoms.

V. DISCUSSION

A. Wills-Harrison transition-metal model

As shown in Fig. 5, the excess vibrational entropy of mixing is negative up to compositions of at least 20% Fe, mostly because of the stiffening of the Au partial phonon DOS. A textbook treatment of Au as a free-electron gas yields a bulk modulus of 35 GPa,[60] but its experimental value is 171 GPa.[61] Hybridization between s and d electrons accounts for the large difference between these values. In the Au-Fe system, there is no correlation between the phonon behavior and the number of electrons at the Fermi level such as in transition-metal alloys,[15,16,24,25] but the behavior can be interpreted with the Wills-Harrison model,[26] which extends the nearly free electron theory of simple metals to include the effects of sd hybridization. Au is a noble metal with fully occupied d states, and our calculations show that the Au partial electronic DOS at each composition retains this noble metal character up to at least 25% Fe. This implies that the 1nn force constants in the low Fe concentration alloys are dominant.

The Wills-Harrison model provides an approximation of the total energy of a metal including contributions from (1) the nearly-free electron gas, (2) hybridization of the s electrons and the d band (using a Friedel model for the d band), and (3) nonorthogonality of hybridized d states (which shifts the center of gravity of the d band). In the notation of Wills and Harrison, these three contributions to the bulk modulus are $B_{\rm fe}$, B_b, and B_c, respectively. The bulk modulus contributions can be obtained by taking the appropriate energy derivatives with respect to volume. The model is based on three parameters. The radius of the empty-core pseudopotential is adjustable, but it is correlated to the core radii calculated from the ionization energy of the atom. The other two, the radius of the atomic volume and the d-state "radius"[62] can be fitted to known values, measured or calculated from first principles. We fitted empty-core pseudopotential radii, while using the values for the other two parameters listed in Ref. 26, to obtain accurate bulk moduli for several elemental transition metals. We then used these parameters to obtain the bulk moduli of alloys of these elements. We observe that $B_{\rm fe}$ is larger for elements towards the middle of the transition metal rows and is particularly small for the noble metals, generally tracking the experimental bulk modulus of each element. The relative weight of $B_{\rm fe}$ remains about the same for elements in the same row, although it decreases with row number. The relative weight of B_c generally increases with row number. As a result, B_c is the most important contribution to the bulk modulus of Au. For Au, $B_{\rm fe} = 55$ GPa, $B_b = -80$ GPa, and $B_c = 195$ GPa. The Wills-Harrison model predicts that the Au-Fe bond is softer than either the Au-Au or Fe-Fe bonds. It also predicts a significant increase in the stiffness of the Au-Au and Fe-Au bonds when the charge is increased. This is not completely offset by the softening of Fe-Fe bonds when the charge is reduced by the same amount. The stiffening of Au-Au bonds with increasing charge comes mostly from changes in B_b.

B. Phonon thermodynamics and electronic structure

The replacement of an Au atom (phonon entropy of fcc Au of 5.64 k_B per atom) with an Fe atom (phonon entropy of fcc Fe, or $Ni_{0.50}{}^{57}Fe_{0.50}$, of 3.50 k_B per atom) can be used to obtain an ideal vibrational entropy of mixing of -2.14 k_B per atom/(at. fraction Fe). However, a fit to the data in Fig. 5 up to 20 at.% Fe gives a slope of -3.75 k_B per atom/(at. fraction Fe), 75% larger than the value from a simple substitution.

The Au partial phonon DOS stiffens considerably with increased Fe concentration, mostly because the Au-Au bonds that have a Fe atom as the nearest neighbor stiffen substantially and this raises the energies of some Au modes above the cutoff energy of pure Au. This is a local effect and the Au atoms that are not close to a Fe atom have force constants that are much closer to that of pure Au, as indicated by our calculations (see Table II). This stiffening trend continues as the Fe concentration is increased and is the main reason why the vibrational entropy of mixing in Fig. 5 is negative at Fe concentrations up to 20%. The magnitude of the excess phonon entropy of mixing is more than half the configurational entropy of mixing and opposite in sign. Although chemical mixing is favored in the fcc phase by the configurational entropy, the phonon entropy favors chemical unmixing, and contributes to the miscibility gap in the Au-Fe phase diagram.[27]

At dilute concentrations, Fe atoms vibrate in a local mode at an energy higher than E_c. Since the 1nn force constants are dominant and Au atoms are four times more massive than the Fe atoms, the Mannheim model can be used to analyze this local mode. This study will be presented elsewhere. With increasing composition there are more Fe atoms in the nearest neighbor shells of other Fe atoms, and this distribution of local environments, which increases linearly with concentration, may be responsible for much of the increase in the peak width of the Fe modes at modest concentrations observed in Fig. 1, which is also linear. The mean energy of this local mode of Fe atoms does not change enough with Fe concentration to have a substantial effect on the vibrational entropy, however.

Figure 3 shows a large increase in the number of Au modes near 8 meV at Fe concentration higher than the percolation limit. This is consistent with an Au resonance mode similar to that observed by Bogdanoff *et al.*[21] in Au-Cu alloys.

The resonance mode of the Au atoms likely increases the phonon entropy on the Fe-rich side of Fig. 5, but data are not available.

Figure 4 shows a sharp peak in Fe 3*d* electrons at the Fermi level of fcc Au-Fe. This peak grows and broadens with increased Fe concentration. The Fe 3*d* electrons at the Fermi level may facilitate the screening of the Fe atom motions,[16,24,25,63] perhaps counteracting somewhat the tendency for phonons to stiffen with the decrease in lattice parameter. Nevertheless, from Fig. 5, we see that the larger effect on the vibrational entropy is from the stiffening of the the vibrations of Au atoms.

The Wills-Harrison model predicts a value of 143 GPa for the bulk modulus of the Fe-Au bond, compared to 174 and 169 GPa for Au-Au and Fe-Fe bonds, respectively. This is in agreement with the *ab initio* calculations, which predict that the Fe-Au bond is softer than the Au-Au bond. For Fe-Au bonds, the relative weight of each contribution, B_{fe}, B_b, and B_c, is intermediate between that of noble metal and transition metal bonds, and B_b and B_c almost cancel each other out. As the Fe concentration increases, the phonon DOS stiffens and both the Au-Au and Fe-Au bonds stiffen (see Table II). This stiffening is predicted by the Wills-Harrison model when charge is added to these bonds and comes mostly from B_b, the coupling between occupied *d* states and empty plane-wave states. The model also predicts an overall increase in the hybridization contribution to the bulk modulus (B_b and B_c) when the lattice parameter is reduced in the case of noble metals. The electronic origin of the change of Au atom stiffness is from *s* states near the Fermi level and from *sd* hybridization. Considering just the free-electron-like contributions, we would expect a stiffening of the Au-Au bonds with Fe concentration for two reasons.

First, there is a charge transfer from Fe to Au. It is difficult to quantify the charge transfer with respect to pure fcc Fe, but the charge in a sphere of radius 1.503 Å about Au atoms in the SQSs that are next to Fe atoms is larger than the charge around Au atoms that are not, indicating a transfer from Fe atoms to each 1nn Au atom of about 0.04 electrons. The electronic DOS of Au in Fig. 4 can be approximated as a band of nearly-free electrons with 0.2 /states/eV/atom at a Fermi level that lies 10 eV above the bottom of the band. For a Fe concentration of 10%, if each Fe atom contributes half an electron to the nearly free electron band, B_{fe} for the Au-Au bonds will increase by 5%.

Second, the lattice parameter is reduced with Fe concentration, giving an increase in nearly-free electron density that is proportional to the modulus. For a Fe concentration of 10%, using the lattice parameters of Table I, this gives an increase of 1.7%. The Au-Au bond bulk modulus stiffening due to free-electron like contributions is therefore 6.7% for a Fe concentration of 10%.

Following the analysis in Ref. 64, we calculated the elastic constants for the Au-Au bonds in pure Au, $Au_{31}Fe_1$, and Au_3Fe from the interatomic force constants given in Table II and we obtained 185, 193, and 246 GPa, respectively, for the bulk modulus. The value for pure Au is in good agreement with experiments.[61] For the Fe-Au bond in $Au_{31}Fe_1$, we obtained 63 GPa. These values come from DFT calculations, so they include all the electronic contributions, including hybridization. The increase in the bulk modulus is linear and predicts a stiffening of the Au-Au bond of 13% at a composition of 10% Fe. We estimated above that about half (6.7%) comes from filling of the nearly free electron band and thus, the other half results from changes in the *sd* hybridization. Assuming the interatomic force constants increase by this total of 13%, Eq. (1) predicts that the vibrational entropy will decrease by $0.20\,k_{\mathrm{B}}$ per atom. This is close to the observed change in Fig. 5, which is about $0.16\,k_{\mathrm{B}}$ per atom.

VI. CONCLUSION

At low Fe concentrations in fcc Au, the vibrational entropy of mixing is smaller than for an ideal solution. Most of this effect is caused by a local stiffening of the Au-Au bonds that are the nearest neighbors of a Fe atom, so the partial phonon DOS stiffens with Fe concentration. The Au motions are more sensitive to Fe concentration than those of Fe. Chemical mixing of the Au and Fe atoms is favored by the configurational entropy, but the vibrational entropy has the opposite sign and contributes to the miscibility gap. The electronic structures of Au-rich Au-Fe alloys show a peak in the electronic DOS from 3*d* electrons at the Fermi level, but we propose a different electronic mechanism responsible for the change in vibrational entropy with alloying. We propose that the Au partial phonon DOS stiffens with Fe concentration owing to the filling of the nearly free band of *s* electrons, and stronger *sd* hybridization. The result is a stiffening of the Au-Au bonds as Fe atoms donate electrons to the Au atoms.

ACKNOWLEDGMENTS

Portions of this work were performed at HPCAT (Sector 16), Advanced Photon Source (APS), Argonne National Laboratory. HPCAT is supported by CIW, CDAC, UNLV, and LLNL through funding from DOE-NNSA, DOE-BES, and NSF. Use of the APS was supported by DOE-BES, under Contract No. DE-AC02-06CH11357. A portion of this research at Oak Ridge National Laboratory's Spallation Neutron Source was sponsored by the Scientific User Facilities Division, Office of Basic Energy Sciences, US Department of Energy. This work benefited from DANSE software developed under NSF Grant No. DMR-0520547. This work was supported by DOE BES under contract DE-FG02-03ER46055.

[1] J. Crangle and W. R. Scott, J. Appl. Phys. **36**, 921 (1965).

[2] S. Mehendale, Y. Girard, V. Repain, C. Chacon, J. Lagoute, S. Rousset, M. Marathe, and S. Narasimhan, Phys. Rev. Lett. **105**, 056101 (2010).

[3] M. Chen, S. Yamamuro, D. Farrell, and S. A. Majetich, J. Appl. Phys. **93**, 7551 (2003).

[4] I.-C. Chiang and D.-H. Chen, Adv. Funct. Mater. **17**, 1311 (2007).

[5]H. L. Liu, J. H. Wu, J. H. Min, and Y. K. Kim, J. Appl. Phys. **103**, 07D529 (2008).

[6]H. Liu, P. Hou, W. Zhang, Y. K. Kim, and J. Wu, Nanotechnology **21**, 335602 (2010).

[7]Y.-N. Wu, D.-H. Chen, X.-Y. Shi, C.-C. Lian, T.-Y. Wang, C.-S. Yeh, K. R. Ratinac, P. Thordarson, F. Braet, and D.-B. Shieh, Nanomed: Nanotechnol **7**, 420 (2011).

[8]E. E. Connor, J. Mwamuka, C. J. M. Anand Gole, and M. D. Wyatt, Small **1**, 325 (2005).

[9]D. G. Howard and R. H. Nussbaum, Phys. Rev. B **9**, 794 (1974).

[10]P. D. Mannheim, Phys. Rev. **165**, 1011 (1968).

[11]B. R. Cuenya, W. Keune, R. Peters, E. Schuster, B. Sahoo, U. von Hörsten, W. Sturhahn, J. Zhao, T. S. Toellner, E. E. Alp, and S. D. Bader, Phys. Rev. B **77**, 165410 (2008).

[12]E. E. Alp, W. Sturhahn, and T. S. Toellner, Hyperfine Interact. **135**, 295 (2001).

[13]B. R. Cuenya, L. K. Ono, J. R. Croy, A. Naitabdi, H. Heinrich, J. Zhao, E. E. Alp, W. Sturhahn, and W. Keune, Appl. Phys. Lett. **95**, 143103 (2009).

[14]B. Fultz, Prog. Mater. Sci. **55**, 247 (2010).

[15]M. S. Lucas, J. A. Muñoz, O. Delaire, N. D. Markovskiy, M. B. Stone, D. L. Abernathy, I. Halevy, L. Mauger, J. B. Keith, M. L. Winterrose, Y. Xiao, M. Lerche, and B. Fultz, Phys. Rev. B **82**, 144306 (2010).

[16]J. A. Muñoz, M. S. Lucas, O. Delaire, M. L. Winterrose, L. Mauger, C. W. Li, A. O. Sheets, M. B. Stone, D. L. Abernathy, Y. Xiao, P. Chow, and B. Fultz, Phys. Rev. Lett. **107**, 115501 (2011).

[17]M. S. Lucas, A. Papandrew, B. Fultz, and M. Y. Hu, Phys. Rev. B **75**, 054307 (2007).

[18]M. S. Lucas, M. Kresch, R. Stevens, and B. Fultz, Phys. Rev. B **77**, 184303 (2008).

[19]M. S. Lucas, J. A. Muñoz, L. Mauger, C. W. Li, A. O. Sheets, Z. Turgut, J. Horwath, D. L. Abernathy, M. B. Stone, O. Delaire, Y. Xiao, and B. Fultz, J. Appl. Phys. **108**, 023519 (2010).

[20]P. D. Bogdanoff, B. Fultz, S. Rosenkranz, and L. Crow, Phys. Rev. B **65**, 014303 (2001).

[21]P. D. Bogdanoff, T. L. Swan-Wood, and B. Fultz, Phys. Rev. B **68**, 014301 (2003).

[22]W. Sturhahn, J. Phys.: Condens. Matter **16**, S497 (2004).

[23]D. L. Abernathy, M. B. Stone, M. J. Loguillo, M. S. Lucas, O. Delaire, X. Tang, J. Y. Y. Lin, and B. Fultz, Rev. Sci. Instrum. **83**, 015114 (2012).

[24]O. Delaire, M. Kresch, J. A. Muñoz, M. S. Lucas, J. Y. Y. Lin, and B. Fultz, Phys. Rev. B **77**, 214112 (2008).

[25]O. Delaire, M. S. Lucas, J. A. Muñoz, M. Kresch, and B. Fultz, Phys. Rev. Lett. **101**, 105504 (2008).

[26]J. M. Wills and W. A. Harrison, Phys. Rev. B **28**, 4363 (1983).

[27]H. Okamoto, T. B. Massalski, L. J. Swartzendruber, and P. A. Beck, Binary Alloy Phase Diagrams, 2nd ed. **1**, 367 (1990).

[28]E. Raub and P. Walter, Z. Metallk. **41**, 234 (1950).

[29]W. B. Pearson, *A Handbook of Lattice Spacings and Structures of Metals and Alloys* (Pergamon Press, New York, New York, 1958), p. 423.

[30]E. R. Jette, W. L. Bruner, and F. Foote, Tr. A. I. M. M. E. **111**, 354 (1934).

[31]B. Window, Phys. Rev. B **6**, 2013 (1972).

[32]E. E. Alp, W. Sturhahn, T. S. Toellner, J. Zhao, M. Hu, and D. E. Brown, Hyperfine Interact. **144-145**, 3 (2002).

[33]M. Seto, Y. Yoda, S. Kikuta, X. W. Zhang, and M. Ando, Phys. Rev. Lett. **74**, 3828 (1995).

[34]W. Sturhahn, T. S. Toellner, E. E. Alp, X. Zhang, M. Ando, Y. Yoda, S. Kikuta, M. Seto, C. W. Kimball, and B. Dabrowski, Phys. Rev. Lett. **74**, 3832 (1995).

[35]W. Sturhahn, Hyperfine Interact. **125**, 149 (2000).

[36]B. Fultz, T. Kelley, J. Lin, J. Lee, O. Delaire, M. Kresch, M. McKerns, and M. Aivazis, Experimental inelastic neutron scattering: Introduction to DANSE, http://docs.danse.us/DrChops/ExperimentalInelasticNeutronScattering.pdf (2009).

[37]M. G. Kresch, Ph.D. thesis, California Institute of Technology, 2009.

[38]M. Kresch, O. Delaire, R. Stevens, J. Y. Y. Lin, and B. Fultz, Phys. Rev. B **75**, 104301 (2007).

[39]J. W. Lynn, H. G. Smith, and R. M. Nicklow, Phys. Rev. B **8**, 3493 (1973).

[40]R. Kikuchi, Phys. Rev. **81**, 988 (1951).

[41]J. M. Sanchez, F. Ducastelle, and D. Gratias, Physica A **128**, 334 (1984).

[42]A. Zunger, S.-H. Wei, L. G. Ferreira, and J. E. Bernard, Phys. Rev. Lett. **65**, 353 (1990).

[43]J. von Pezold, A. Dick, M. Friák, and J. Neugebauer, Phys. Rev. B **81**, 094203 (2010).

[44]G. Kresse and J. Furthmüller, Phys. Rev. B **54**, 11169 (1996).

[45]G. Kresse and J. Furthmüller, Comput. Mater. Sci. **6**, 15 (1996).

[46]D. M. Ceperley and B. J. Alder, Phys. Rev. Lett. **45**, 566 (1980).

[47]J. P. Perdew and A. Zunger, Phys. Rev. B **23**, 5048 (1981).

[48]H. J. Monkhorst and J. D. Pack, Phys. Rev. B **13**, 5188 (1976).

[49]B. Grabowski, T. Hickel, and J. Neugebauer, Phys. Rev. B **76**, 024309 (2007).

[50]K. Parlinski, Z. Q. Li, and Y. Kawazoe, Phys. Rev. Lett. **78**, 4063 (1997).

[51]A. Togo, F. Oba, and I. Tanaka, Phys. Rev. B **78**, 134106 (2008).

[52]A. A. Quong, Phys. Rev. B **49**, 3226 (1993).

[53]X. Tang and B. Fultz, Phys. Rev. B **84**, 054303 (2011).

[54]D. C. Wallace, *Statistical Physics of Crystals and Liquids* (World Scientific, Singapore, 2002).

[55]M. S. Lucas, L. Mauger, J. A. Muñoz, Y. Xiao, A. O. Sheets, S. L. Semiatin, J. Horwath, and Z. Turgut, J. Appl. Phys. **109**, 07E307 (2011).

[56]M. S. Lucas, L. Mauger, J. A. Muñoz, I. Halevy, J. Horwath, S. L. Semiatin, M. B. Stone, D. L. Abernathy, Y. Xiao, P. Chow, and B. Fultz, J. Appl. Phys. (in press).

[57]Y. Tsunoda, Y. Kurimoto, M. Seto, S. Kitao, and Y. Yoda, Phys. Rev. B **66**, 214304 (2002).

[58]T. Tanaka, A. Tajima, R. Moriizumi, C. Oshima, Y. Tsunoda, M. Seto, S. Kitao, and T. Mitsui, J. Phys. Soc. Jpn. **74**, 1762 (2005).

[59]J. Zarestky and C. Stassis, Phys. Rev. B **35**, 4500 (1987).

[60]N. W. Ashcroft and N. D. Mermin, *Solid State Physics* (Holt, Rinehart and Winston, New York, 1976), p. 38.

[61]C. J. Smithells and G. B. Brook, in *Smithells Metals Reference Book*, 7th ed., edited by E. A. Brandes and G. B. Brook (Butterworth-Heinemann, Jordan Hill, Oxford, 1992), p. 2.

[62]W. A. Harrison and S. Froyen, Phys. Rev. B **21**, 3214 (1980).

[63]O. Delaire, K. Marty, M. B. Stone, P. R. C. Kent, M. S. Lucas, D. L. Abernathy, D. Mandrus, and B. C. Sales, Proc. Natl. Acad. Sci. USA **108**, 4725 (2011).

[64]B. E. Warren, *X-ray Diffraction* (Addison-Wesley, Menlo Park, CA, 1969), p. 178.